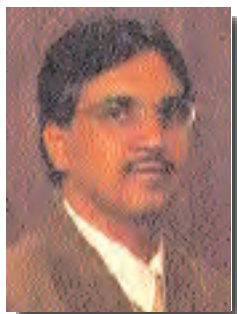


Flexural Response of CFRP Prestressed Concrete Box Beams for Highway Bridges



Nabil F. Grace, Ph.D., P.E.
Professor and Chairman
Civil Engineering Department
Lawrence Technological University
Southfield, Michigan



S. B. Singh, Ph.D.
Research Engineer
Civil Engineering Department
Lawrence Technological University
Southfield, Michigan



Mina M. Shinouda
Graduate Student
Civil Engineering Department
Lawrence Technological University
Southfield, Michigan



Sunup S. Mathew
Graduate Student
Civil Engineering Department
Lawrence Technological University
Southfield, Michigan

This paper presents an experimental and analytical investigation of the flexural response of box beams reinforced and prestressed using carbon fiber reinforced polymer (CFRP) tendons. Two one-third scale box beams were prestressed using seven bonded pretensioning tendons and six unbonded post-tensioning tendons. A third beam was prestressed with seven bonded pretensioning tendons and six non-prestressed unbonded post-tensioning tendons. Beams were reinforced with carbon fiber composite cable stirrups and tested to failure. A computer program was developed to predict deflection, strain, and post-tensioning forces at various loads. A parametric analysis examined the effects of the level of pretensioning and post-tensioning forces on the overall flexural response. Results showed that the beam prestressed using both pretensioning and unbonded post-tensioning tendons had a 26 percent higher ultimate load capacity and 36 percent lower energy ratio than the beam with non-prestressed unbonded post-tensioning tendons. Levels of initial pretensioning and post-tensioning forces significantly affect the flexural response and beam failure mode.

Current research is being conducted worldwide to explore the suitability and efficiency of non-corrodible advanced fiber reinforced polymers (FRPs) such as carbon fiber reinforced polymer (CFRP) and aramid fiber reinforced polymer (AFRP) for reinforcing and prestressing of concrete structures.¹ Corrosion of reinforcing steel bars has been a major concern for concrete structures, especially in

cold and marine climates, where deicing salts and aggressive environmental conditions have led to severe structural deterioration.

Advanced fibrous composite materials, especially CFRP, have important material characteristics such as non-corrosiveness, high strength, high stiffness-to-weight ratios, light weight, and insensitivity to magnetic effects. These desirable properties make FRP a construction material of great potential to alleviate corrosion, reduce structural maintenance, and improve production efficiency.

FRP materials, however, do exhibit one major disadvantage: they are linearly elastic until failure and, unlike steel, they are brittle in nature. It, therefore, is essential to investigate the overall response and ductility of structures reinforced and prestressed using CFRP tendons and strands prior to their large-scale use in construction.

BACKGROUND

Naaman et al.² examined the flexural behavior of concrete beams partially prestressed with CFCC strands and concluded that non-prestressing steel reinforcing bars can help in providing residual strength and ductility. In that study, the failure of prestressing tendons occurred after yielding of steel reinforcing bars. Naaman also concluded that the conventional methods of equilibrium, strain compatibility, and material constitutive relationships could be used to predict the flexural responses of fully or partially prestressed beams using CFCC strands.

Yonekura et al.³ examined the effects of the type and quantity of pretensioning tendons, axial reinforcement, and the level of initial prestressing forces on the flexural response of concrete I-beams prestressed using AFRP and CFRP tendons. They observed that the deflection of concrete beams reinforced and prestressed using FRP tendons is greater than that of beams using steel reinforcing bars.

Based on experimental and analytical evaluation of flexural deformation in rectangular and T-sections, Abdelrahman et al.⁴ concluded that CFRP prestressed concrete structures should be designed to exhibit considerable deformation and crack formation before ultimate failure. Zou et al.⁵ studied the load-deflection response, residual deformation, and ductility of two CFRP prestressed concrete rectangular cross-sectional beams. Load-deflection behavior of the tested beams was found to be bilinear with reduced post-cracking stiffness. Deflection corresponding to the ultimate failure load of the beam was observed to decrease with increase in concrete strength.

In addition to the above studies on the response of pre-

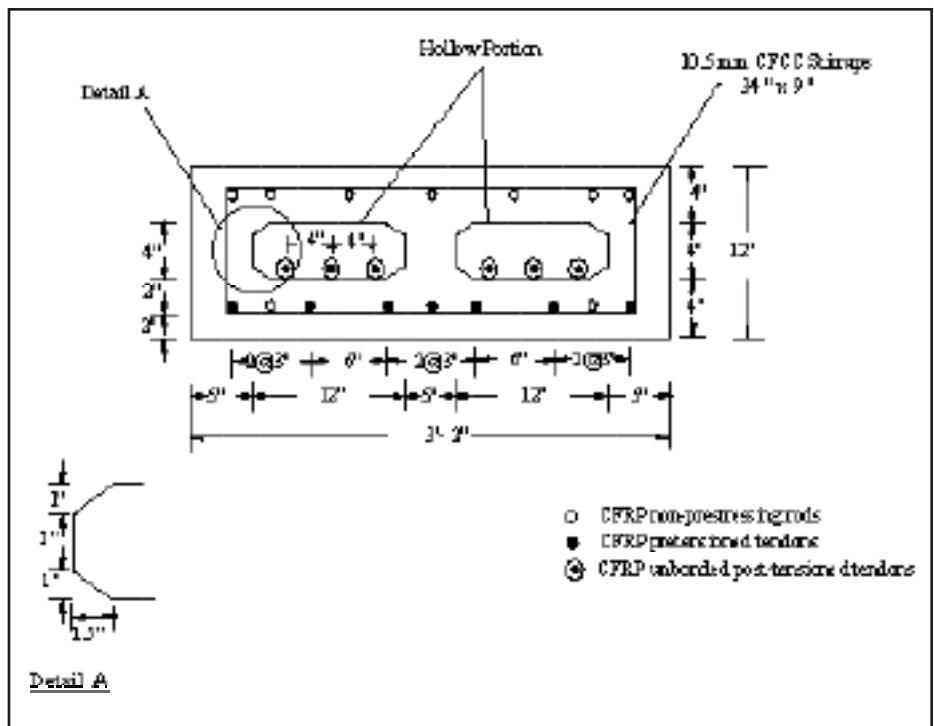


Fig. 1. Cross-sectional details of tested box beam.

stressed concrete structures, Kato and Hayashida⁶ studied the flexural characteristics of concrete beams prestressed independently with bonded and unbonded CFRP tendons. They concluded that the failure mode of concrete beams prestressed using bonded pretensioning tendons was brittle, whereas beams prestressed with unbonded CFRP post-tensioning tendons had roughly the same degree of ductility as that of beams reinforced with steel reinforcing bars.

Maissen and de Semet⁷ compared the behavior of concrete beams prestressed using CFRP bonded and unbonded tendons with that of beams prestressed with bonded steel strands. They concluded that the flexural capacity of beams prestressed with unbonded tendons was greater than that of a beam prestressed with bonded tendons. From the study by Naaman and Jeong⁸ on the structural ductility of concrete beams prestressed with AFRP, CFRP, and steel strands, it was concluded that the beams prestressed with FRP tendons had considerably lower ductility than beams prestressed with steel strands.

A new proposed construction approach^{9,10} for multi-span CFRP prestressed concrete bridges demonstrated that external post-tensioning using draped tendons, continuity design of deck slab, and transverse post-tensioning increases the ductility of the bridge system. Recently, Grace and Singh^{11,12} proposed a unified analysis and design approach for CFRP prestressed concrete bridge beams; this approach uses bonded pretensioning and unbonded post-tensioning tendons arranged in multiple, vertically distributed layers along with non-prestressing CFRP rods.

The design approach of Grace and Singh¹¹ was validated by comparing the analytical and experimental results (Grace et al.¹³) of a full-scale double-tee (DT) beam. This DT beam was similar to those used in the Bridge Street Bridge,¹⁴ City

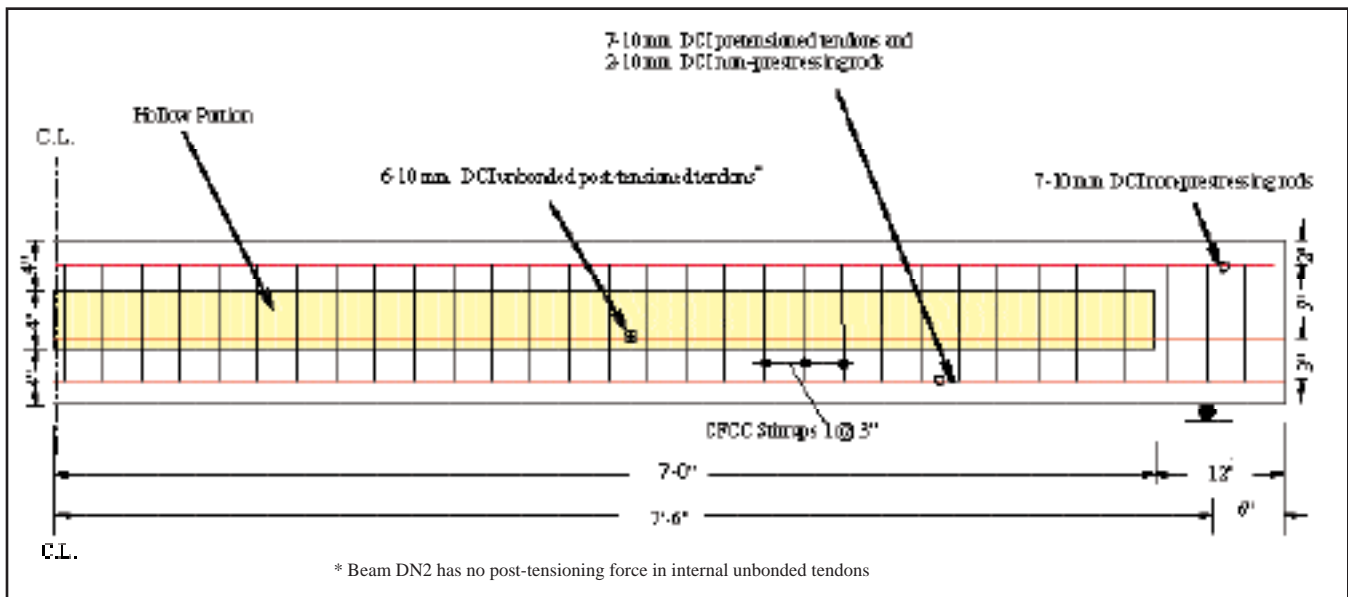


Fig. 2. Typical reinforcement details of box beams (Beam DP1 is shown).

Table 1. Properties of CFRP materials.

| | CFRP tendons | Leadline™ tendons | CFCC strand |
|---|--|---|--------------------------|
| Manufacturer | Diversified Composites, Inc. (DCI) ¹⁵ | Mitsubishi Chemical Corporation (MCC) ¹⁶ | Tokyo Rope ¹⁷ |
| Nominal diameter, <i>d</i> , in. (mm) | 0.374 (9.5) | 0.394 (10.0) | 0.41 (10.5) |
| Effective cross-sectional area, sq in. (mm ²) | 0.11 (70.9) | 0.122 (78.7) | 0.086 (55.7) |
| Guaranteed strength, ksi (MPa) | 221 (1524) | 328 (2262) | 271 (1869) |
| Ultimate tensile strength, ksi (MPa) | 280 (1931) | 415 (2861) | 305 (2103) |
| Elastic modulus, ksi (GPa) | 19,000 (131) | 21,320 (147) | 19,865 (137) |
| Maximum percent elongation | 1.47 | 1.9 | 1.5 |

of Southfield, Michigan. From these studies, it was concluded that the combination of bonded and unbonded prestressing levels (0.3 to 0.6) could significantly increase the moment capacity of an over-reinforced beam. The over-reinforced beam is based on both the prestressing and unbonded post-tensioning tendons.¹¹

The above investigations indicate that flexural responses of CFRP reinforced beams prestressed using bonded and unbonded tendons have not been examined in detail. Moreover, there is no known published literature dealing with the flexural response of a box beam prestressed using bonded prestressing and unbonded post-tensioning tendons arranged in vertically distributed layers.

The aim of the present investigation is to examine the flexural response of box beams reinforced with CFRP rods and stirrups, and prestressed using internal bonded and unbonded tendons arranged in three layers along the cross-sectional depth of the box beam. The variation of deflections, strains, and post-tensioning forces with applied loading are presented, including the ultimate load-carrying capacity. Recommendations based on the parametric study using the developed computer program are also presented.

CONSTRUCTION DETAILS

A total of three one-third-scale box beams designed to fail in flexure were constructed. Each box beam was 16 ft (4.9 m) long, 38 in. (965 mm) wide, and 12 in. (305 mm) deep (see Fig. 1). Two beams were prestressed using seven bonded prestressing and six unbonded post-tensioning tendons. One of the two box beams was prestressed using 0.374 in. (9.5 mm) diameter Diversified Composites, Inc. (DCI) tendons,¹⁵ and the second beam was prestressed using 0.394 in. (10 mm) diameter Leadline™ tendons.* The third beam was prestressed with seven 0.374 in. (9.5 mm) bonded DCI prestressing tendons and used six non-prestressed unbonded DCI post-tensioning tendons with anchor heads at both ends of the beam. All three box beams were reinforced with 0.41 in. (10.4 mm) carbon fiber composite cable (CFCC)¹⁷ stirrups.

Beams were designated as Beams DP1, DN2, and LP3. Beam DP1 was prestressed using bonded and unbonded DCI tendons; Beam DN2 was prestressed using only bonded prestressing DCI tendons with non-prestressed unbonded tendons installed in the beam; and Beam LP3 was prestressed using bonded prestressing and unbonded post-tensioning Leadline tendons.

Fig. 2 shows the typical reinforcement details of tested Box Beam DP1 reinforced symmetrically with respect to the midspan section. The other tested box beams were rein-

forced in the same manner. As indicated in Fig. 2, the center-to-center distance between the supports was 15 ft (4.6 m). The material properties of the DCI CFRP tendons, Leadline tendons, and CFCC strands[†] used for reinforcing and prestressing of the box beams are presented in Table 1. Details of prestressing forces, number and type of tendons used in prestressing, ultimate failure loads, and energy ratio of Box Beams DP1, DN2, and LP3 are presented in Table 2. The energy ratio¹⁰ is defined as the ratio of inelastic energy absorbed in the structural system to the total energy of the system.

Prestressing

CFRP prestressing tendons were provided with a special mechanical anchorage system at each end to facilitate pulling of the tendons without damaging their ends. This anchorage system consisted of a metal tube, sleeve, and steel wedge. Tendons were degreased with acetone over a length of 6 in. (152 mm) from the end and inserted in the metal tube that was fitted into the groove between two halves of the wedge. A tapered piece of Teflon tape was wrapped around the wedge before pushing it into the anchor by use of a center-hole hydraulic jack.

The prestressing equipment consisted of a long-stroke, center-hole hydraulic jack, hydraulic pump with a pressure gauge, and a prestressing chair to stress each tendon in sequence. Lock nuts were tightened over the anchors after prestressing each tendon with a spacer placed between the bulkhead and locknut (see Fig. 3).

Load cells (placed at the dead end of the beams) were used to monitor the forces in each prestressing tendon. Each prestressing tendon was pulled to an average load of 20.8 kips (92.5 kN), which is about 86 and 41 percent of breaking load of DCI and Leadline tendons, respectively. Concrete was placed immediately after pretensioning of the tendons.

Four prestressing bulkheads fixed to the floor were used in the pretensioning of the tendons to allow the fabrication of two beams at a time. Tendons were released by cutting them using a hand-held saw after the concrete achieved the

Table 2. Details of prestressing forces and failure loads of box beams.

| Beam | Number and type of tendons used in prestressing | | Total prestressing force, kips (kN) | f'_c , ksi (MPa) | Ultimate load, kips (kN) | Energy ratio, percent |
|------|--|---|-------------------------------------|--------------------|--------------------------|-----------------------|
| | Pre-tensioning | Post-tensioning | | | | |
| DP1 | 7 DCI ¹⁵ tendons | 6 DCI ¹⁵ tendons | 271 (1206) | 7.0 (48.3) | 86 (383) | 32 |
| DN2 | 7 DCI ¹⁵ tendons | 6 DCI ¹⁵ tendons without post-tensioning | 147 (654) | 7.0 (48.3) | 69 (307) | 50 |
| LP3 | 7 MCC ¹⁶ Leadline TM tendons | 6 MCC ¹⁶ Leadline TM tendons | 270 (1202) | 7.0 (48.3) | 99 (440) | 33 |

Note: All three box beams failed in flexure.

desired compressive strength (see Fig. 4). Prestressing of unbonded post-tensioning tendons was completed seven days after the concrete placement. Load cells installed at the dead end of the beam measured forces in the unbonded post-tensioning tendons during post-tensioning and during the load test.

INSTRUMENTATION AND TEST SETUP

A total of 15 strain gauges were installed on the midspan concrete surface to monitor the concrete strain in the box beams. Five of the 15 strain gauges were placed at the top concrete surface and five gauges were installed on each side of the beam. The midspan deflection of the box beams was measured using string pots fixed to a stationary strut and at-

* LeadlineTM tendons are manufactured by Mitsubishi Chemical Functional Products, Inc., Japan.

† CFCC strands are manufactured by Tokyo Rope Mfg. Co. Ltd., Japan.

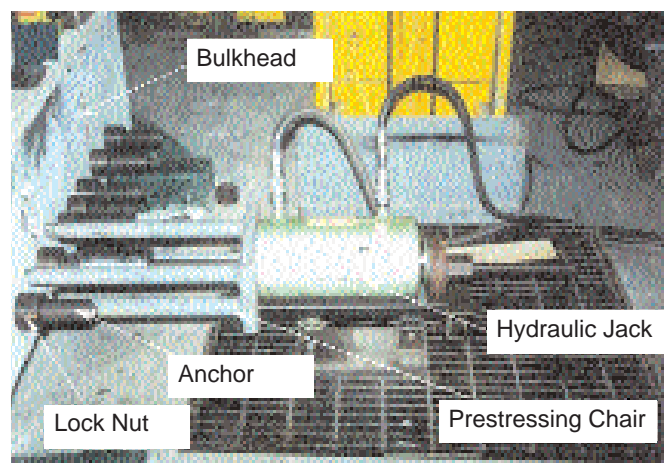


Fig. 3. Prestressing of tendons at live end of box beam.



Fig. 4. Release of prestressing tendons with hand-held saw.

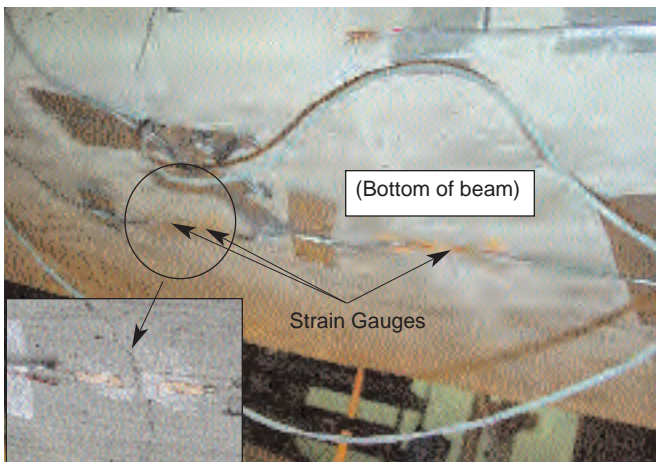


Fig. 5. At the bottom of the beam, strain gauges installed on either side of the first initiated crack for measurement of decompression load.

tached to the top surface of the beams at quarter and midspan sections. A set of four strain gauges was installed adjacent to the first initiated crack during the load test, to predict the decompression load (see Fig. 5). Measurement of the decompression load was necessary to estimate the effective prestress in the pretensioning tendons.

For the examination of overall load deflection, strains, forces in unbonded post-tensioning tendons, and ultimate load responses of the beams, all three box beams were simply supported with an effective span of 15 ft (4.7 m). Each end support had a length equal to the width of the box beams and was resting on another steel support. A jacking force of 200 kips (890 kN) and a hydraulic pump were used to load the entire width of the beam using a four-point loading frame.

Steel plates lined with rubber sheets were used at the two load points and the two supports to evenly distribute the load throughout the width of the beam. Fig. 6 shows the flexural test setup. The longitudinal center-to-center distance between the loading points was 20 in. (508 mm). All sensors including strain gauges and string pots were connected to the data acquisition system, which was used to monitor all the readings throughout the entire testing. All three box beams tested in flexure were subjected to loading and unloading cycles before the ultimate loading.

The beams were first loaded to 40 kips (178 kN), which was less than the cracking load, and then unloaded. Two more loading cycles were applied to the beams before finally loading to failure. The loading and unloading sequence applied to the box beams before ultimate loading was necessary to evaluate the inelastic energy absorbed in the box beams and energy ratio as a measure of ductility index of the CFRP reinforced and prestressed concrete box beams.

THEORETICAL APPROACH AND ANALYSIS

The experimental verification of the analytical results obtained using a special-purpose nonlinear computer program for box beams is presented in this section. This nonlinear computer program for the analysis of the prestressed con-

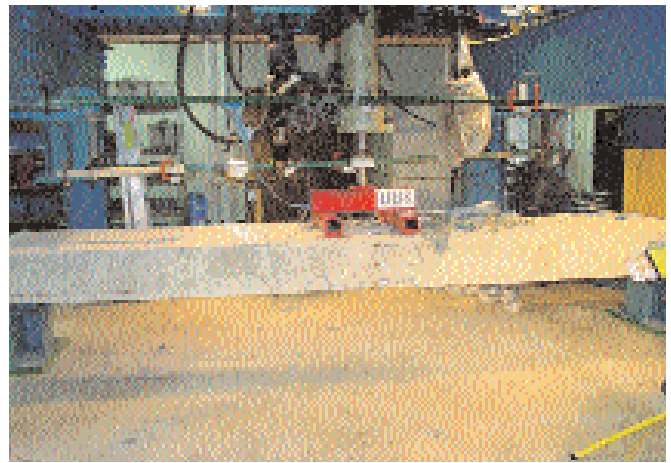


Fig. 6. Flexural test setup of box beam. Box beams are simply supported with a span of 15 ft (4.7 m).

crete box beam was developed using a similar approach presented elsewhere^{11,12} for the analysis of CFRP prestressed concrete DT beams.

Experimental load-versus-strain relationships for the three box beams are presented in order to estimate their decompression loads and the effective prestress in the corresponding pretensioned tendons.

The decompression load is the applied load at the time the precompression in the tensile zone of the beam cross section is completely lost. As described later, this loading point can be predicted fairly accurately using the applied load-versus-strain diagram.

The program incorporates a parabolic stress-strain relationship for concrete and linear stress-strain relationships for CFRP tendons. The compressive force in concrete, however, is computed using equivalent rectangular stress block factors. Rectangular stress block factors¹¹ depend on the level of extreme compression fiber strain and the parabolic stress-strain relationships of concrete. The resultant compression force consists of forces in the concrete and forces in the CFRP rods in the compression zone.

The incremental strain controlled approach was used to predict the neutral axis depth, strains, and curvatures at pre-selected sections along the length of the beams. Fig. 7 shows the distribution of concrete strains, stresses, and resultant forces along the depth of an over-reinforced box beam cross section (reinforcement ratio $\rho/\rho_b > 1$). Midspan deflections were computed by integrating the curvature of the box beam along its length.

A parametric study was conducted to show the effect of the level of initial pretensioning and post-tensioning forces on the overall flexural response, ultimate load-carrying capacity, and failure mode of the box beam. The effect of the level of pretensioning forces on the ratio of actual reinforcement ratio (ρ) and balanced ratio (ρ_b) was also examined.

For the sake of completeness, the expression for reinforcement ratio¹¹ based on tendons arranged in vertically distributed layers is given on the next page. This expression is obtained using the equilibrium of forces and the compatibility of strains in the cross section.

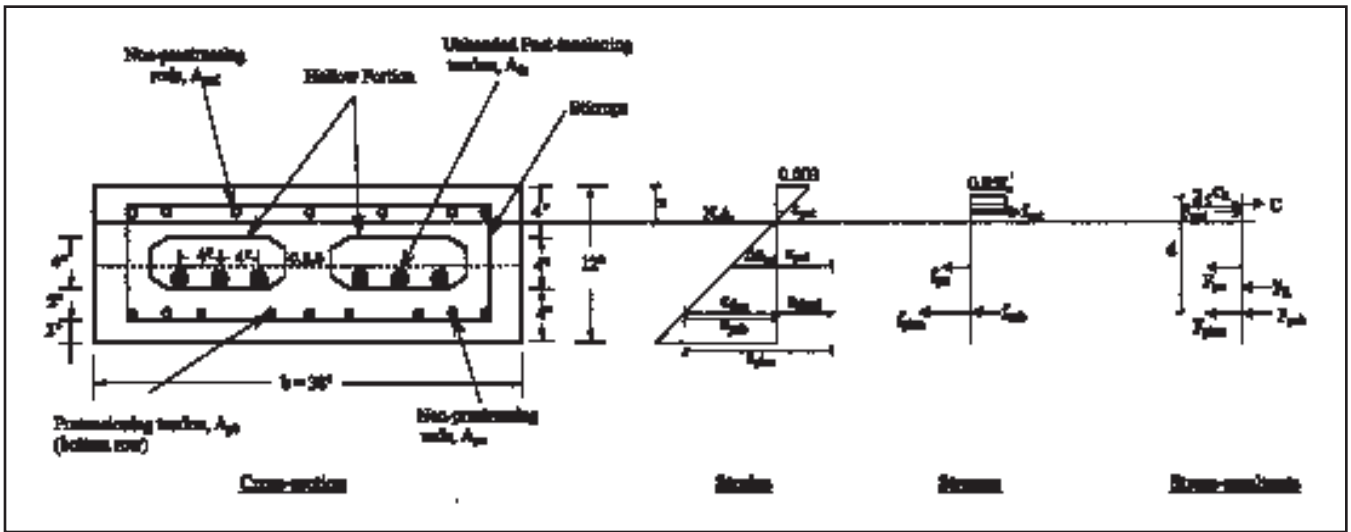


Fig. 7. Strain and stress distributions for over-reinforced box beam.

$$\rho = \frac{\sum_{i=1}^p A_{fi} \alpha_i}{b d_m} \quad (1)$$

$$= \frac{F_{pi} + f_{pbb} A_{pb} + f_{pmbb} A_{pm} + F_{pui} + f_{pub} A_{fu} - f_{pmfb} A_{pmf}}{b d_m f_{fu}}$$

where

$$\alpha_i = \frac{f_{bi}}{f_{fu}}$$

- A_{fi} = cross-sectional area of reinforcement of a particular material (positive for tension reinforcement and negative for compression reinforcement)
- A_{fu} = total cross-sectional area of post-tensioning tendons
- A_{pb} = total cross-sectional area of prestressing bonded tendons
- A_{pm} = total cross-sectional area of non-prestressing tendons provided in tension zone
- A_{pmf} = total cross-sectional area of non-prestressing tendons provided in compression zone
- b = width of box beam
- d_m = distance of centroid of bottom prestressing tendons from extreme compression fiber
- f_{bi} = total stress in an equivalent tendon of a specific material at balanced condition
- f_{fu} = specified tensile strength of bonded prestressing tendons
- f_{pbb} = flexural stress in equivalent bonded prestressing tendons at balanced condition
- f_{pmbb} = flexural stress in equivalent non-prestressing tendons of tension zone at balanced condition
- f_{pmfb} = flexural stress in equivalent non-prestressing tendons of compression zone at balanced condition
- f_{pub} = flexural stress in equivalent unbonded tendons at balanced condition

- F_{pi} = resultant initial effective prestressing force
- F_{pui} = resultant initial effective post-tensioning force
- m = total number of layers of bonded prestressing tendons ($m = 1$, in this case)
- p = total number of reinforcing materials

The above reinforcement ratio is compared with the balanced ratio¹¹ (ρ_b) to classify the section into under-reinforced, balanced, and over-reinforced sections. The failure of an under-reinforced box beam occurs due to rupture of prestressing tendons, whereas that of an over-reinforced beam occurs due to crushing of concrete in the compression zone. The section having a reinforcement ratio (ρ) greater than ρ_b is defined as over-reinforced, while that having ρ greater than $0.5\rho_b$ but less than ρ_b is defined as under-reinforced.

The section having a reinforcement ratio equal to ρ_b is defined as balanced, whereas that having ρ less than $0.5\rho_b$ is defined as significantly under-reinforced. The expression for the balanced ratio is given below. It should be noted that Eq. (2) is based on the equilibrium condition of a balanced section and assumes that the bottom-most prestressing tendons are susceptible to rupture earlier than unbonded post-tensioning tendons or non-prestressing tendons, and works in conjunction with Eq. (1) in defining the section as significantly under-reinforced, under-reinforced, balanced, and over-reinforced.

Eq. (1) represents the actual tensile reinforcement ratio expressed with respect to concrete area covering the depth to the bottom-most prestressing tendons and takes into account the area of bonded and unbonded tendons and non-prestressing rods in tension and compression zones.

$$\rho_b = 0.85 \beta_1 \frac{f'_c}{f_{fu}} \frac{\epsilon_{cu}}{\epsilon_{cu} + \epsilon_{fu} - \epsilon_{pbmi}} \quad (2)$$

where

- β_1 = factor defined as the ratio of the depth of equivalent rectangular stress block to the distance from the extreme compression fiber to the neutral axis

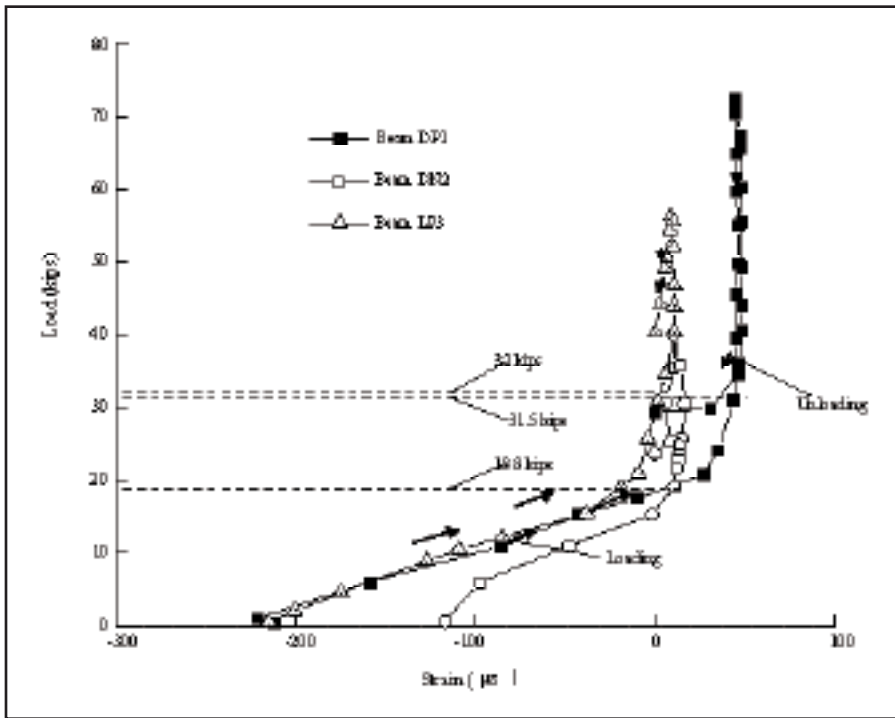


Fig. 8. Concrete strain-versus-loading graph for the bottom flange at box beam midspan. Decompression loads are shown for test beams.



Fig. 9. Flexural failure of Box Beam DP1.

- f'_c = specified compressive strength of concrete
- f_{fu} = specified tensile strength of bonded prestressing tendons
- ϵ_{cu} = ultimate compressive strain in concrete (0.003)
- ϵ_{fu} = specified ultimate strain of pretensioning tendons
- ϵ_{pbmi} = initial prestressing strain in bonded prestressing tendons of m th row (bottom row)

Effective Prestress

To determine the actual effective prestress in the pretensioning tendons, the decompression load was predicted using load-strain relationships for the tested box beams (see Fig. 8). From the load-strain relationship, the decompression load is predicted as the load (when pre-compression in the beam tensile zone is lost) beyond which no further increase in the strain occurs.

The strain readings were obtained from the strain gauges installed adjacent to the first developed crack on the bottom flange of the beam (see Fig. 5). While installing the gauges, load was held constant, but the loading was resumed after the gauges were connected to the data acquisition system to gather the load-versus-strain readings.

As shown in Fig. 8, the predicted decompression loads for Beams DP1, DN2, and LP3 are 31.5, 18.8,

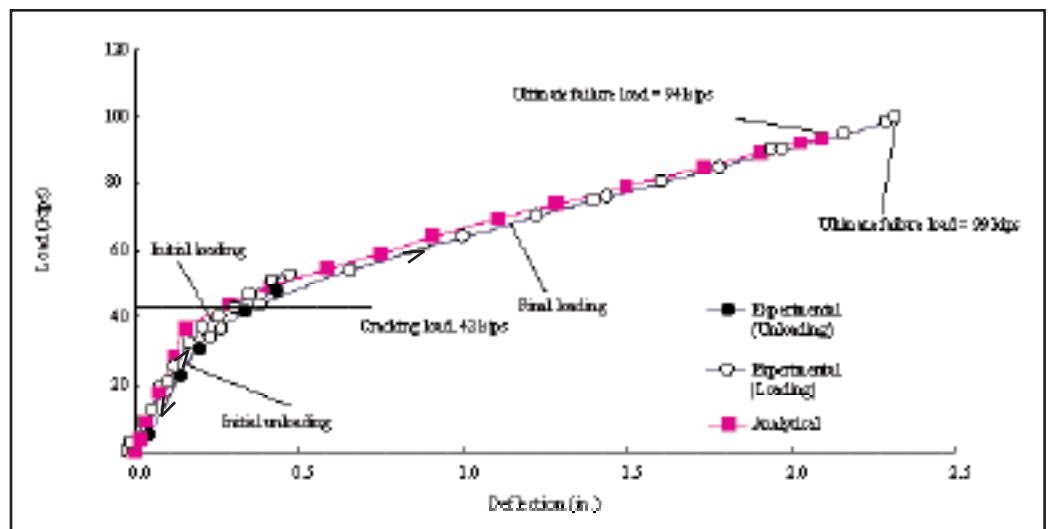


Fig. 10. Load versus midspan deflection of Box Beam LP3.

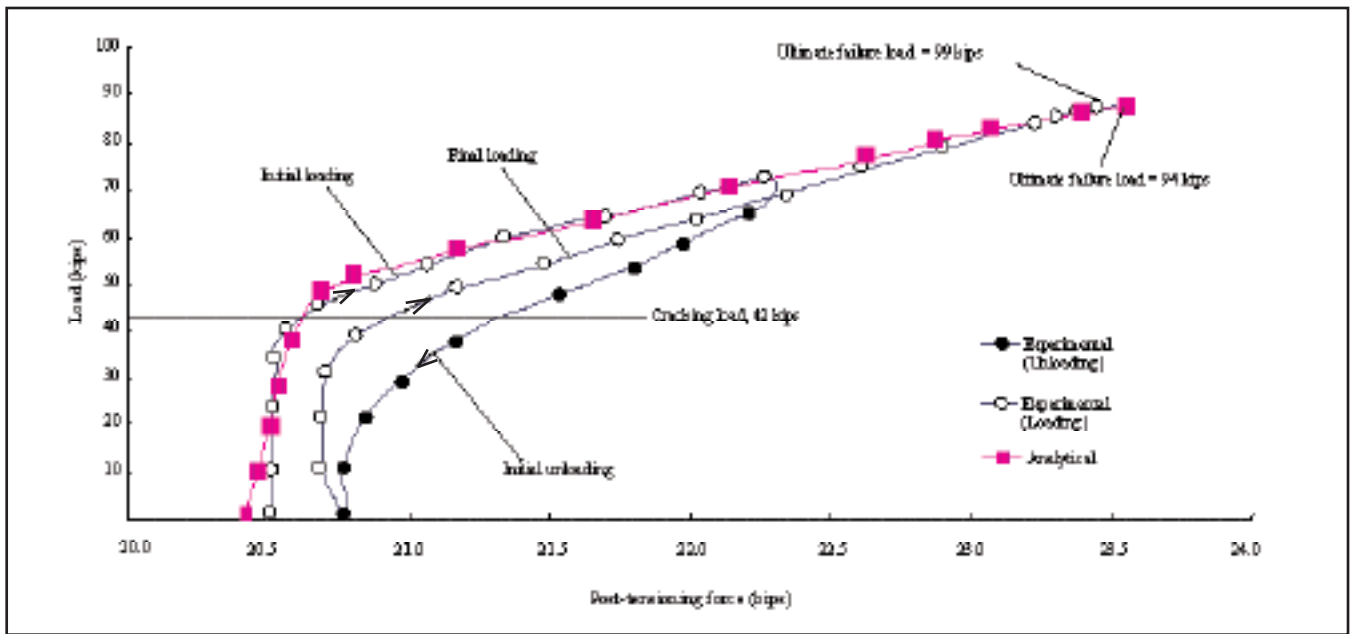


Fig. 11. Load versus post-tensioning force of Box Beam LP3.

and 32.0 kips (140, 83.6 and 142 kN), respectively. The lower value of decompression load for Beam DN2 is due to a lower level of total prestressing force (pre-tensioning plus post-tensioning), about 54 percent of Beams DP1 and LP3.

Total prestress loss for each beam was computed using a back calculation method, wherein decompression loads were used to calculate actual stress at the bottom of the beam due to effective prestress. The computed prestress losses in pre-tensioning forces were 13.6, 8.3, and 10.5 percent for Beams DP1, DN2, and LP3, respectively. Beam DN2 experienced the lowest losses.

This was expected since the presence of post-tensioning forces contributed to the additional elastic shortening of the beam.

The total prestress loss in Beams DP1 and LP3 accounted for the prestressing forces in the unbonded post-tensioning tendons. All three box beams failed in flexure. As expected, the beams prestressed using both the pre-tensioning and post-tensioning tendons had higher load-carrying capacity in comparison to that of Beam DN2 prestressed using pre-tensioning tendons only with non-prestressed unbonded post-tensioning tendons installed in the beam. Table 2 lists the failure loads of Beams DP1, DN2, and LP3 as 86, 69, and 99 kips (383, 307, and 440 kN), respectively.

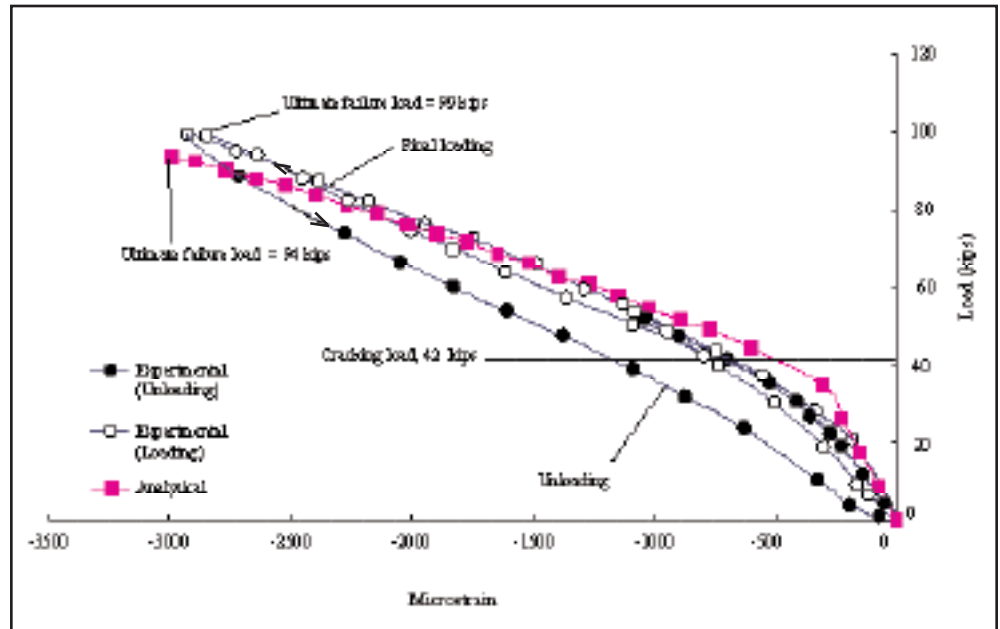


Fig. 12. Load versus strain in top flange (extreme fiber) at midspan of Box Beam LP3.

Results revealed that the Leadline tendons are more effective than DCI tendons with regard to improving the load-carrying capacity of beams. This is attributed to the higher tensile strength of the Leadline tendons compared to the DCI tendons. The typical flexural failure of Beam DP1 is shown in Fig. 9. Note that the tested beams did not collapse suddenly to the ground, but remained suspended between supports. In fact, the presence of the external post-tensioning tendons helped in restraining the beam from sudden collapse even after the rupture of pre-tensioning tendons. The failure of the pre-tensioning tendons was abrupt, and the post-tensioning tendons were intact even after the ultimate failure of the beam.

Table 3. Comparison of analytical and experimental results.

| Beam | Analytical results | | | Experimental results | | |
|------|--------------------------|-------------------------|----------------------|--------------------------|-------------------------|----------------------|
| | Cracking load, kips (kN) | Failure load, kips (kN) | Deflection, in. (mm) | Cracking load, kips (kN) | Failure load, kips (kN) | Deflection, in. (mm) |
| DP1 | 38 (169) | 87 (387) | 2.70 (69) | 38 (169) | 86 (383) | 2.56 (65) |
| DN2 | 28 (125) | 66 (294) | 2.60 (66) | 20 (89) | 69 (307) | 2.88 (73) |
| LP3 | 42 (187) | 94 (418) | 2.20 (56) | 42 (187) | 99 (441) | 2.31 (59) |

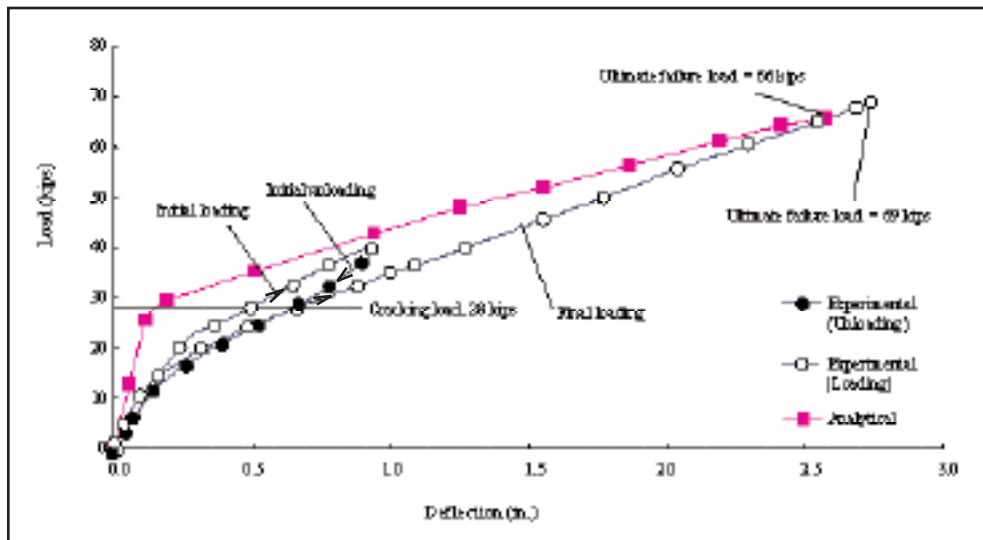


Fig. 13. Load versus midspan deflection of Box Beam DN2.

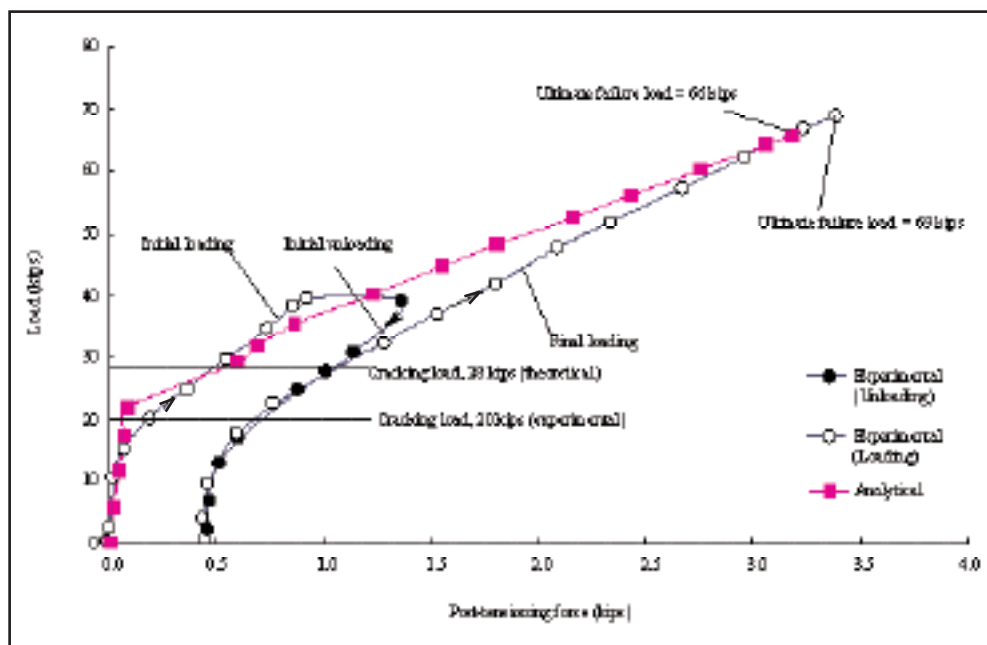


Fig. 14. Load versus force developed in post-tensioning tendons of Box Beam DN2.

The energy ratios for Beams DP1, DN2, and LP3 were 32, 50, and 33 percent, respectively (see Table 2). The higher level of ductility for Beam DN2 is due to early rupture of bonded pretensioning tendons followed by delayed crushing of concrete, giving additional inelastic energy to the beam.

The low energy ratio of the beams prestressed using both the bonded pretensioning and unbonded post-tensioning tendons was due to under-reinforced box beam sections. Designing over-reinforced sections can alleviate the premature failure of bonded tendons before compression failure of concrete and could increase the ductility of the beam.¹⁰

Experimental Verification

The comparison of the analytical load versus deflection, post-tensioning forces in unbonded post-tensioning tendons, and extreme fiber compressive strains at midspan with corresponding experimental results, obtained from testing of Beam LP3, is presented in Figs. 10, 11, and 12, respectively. It is observed that the analytical and experimental load versus deflection (Fig. 10), load versus post-tensioning force (Fig. 11), and load versus extreme fiber compressive strain (Fig. 12) relationships are in fair agreement. The cracking and ultimate loads of the box beams are marked in the figures.

A slight difference in the experimental and analytical results occurred in the advanced post-cracking stage of deformation, and is due to the experimental loading and

unloading cycles applied to the tested beams prior to the ultimate load test and also due to assumptions made in the equations. The percentage difference in the experimental and analytical ultimate load-carrying capacities of Beam LP3 is about 5 percent. Similar comparative responses were

obtained for Beam DP1, also with almost negligible difference in the analytical and experimental load-carrying capacities of the box beams (see Table 3).

As shown in Figs. 13 and 14, the difference in the experimental and analytical responses of Beam DN2 (beam with non-prestressed unbonded post-tensioning tendons) is also not significant. This difference in the analytical and experimental responses of Beam DN2, however, is slightly larger in comparison to the corresponding responses of Beams DP1 and LP3. The maximum effect of loading and unloading cycles on the difference in the experimental and analytical responses of box beams is observed on the load-versus-strain relationships of Beam DN2 (see Fig. 15).

Parametric Study

To examine the effect of the level of pretensioning and post-tensioning forces on the flexural response and ultimate load-carrying capacity of box beams, the calculated load-versus-deflection responses (of box beams prestressed and reinforced with DCI tendons) are presented in Figs. 16 and 17. For a particular level of prestressing forces in unbonded post-tensioning tendons ($upl = 0.7$), the level of pretensioning forces (bpl) has a significant effect on the load-deflection response of the beam. Here, bpl refers to the ratio of prestress in the bonded pretensioning tendons to the specified tensile strength of pretensioning tendons, whereas upl refers to the ratio of prestress in unbonded post-tensioning tendons to the specified tensile strength of unbonded tendons.

Fig. 16 illustrates that variation in the level of pretensioning forces will result in different reinforcement and balanced ratios of the box beam provided with the same pretensioning tendons and non-prestressing rods. The ratio of reinforcement to balanced ratios (ρ/ρ_b) along with the ultimate load-carrying capacity of the box beam is shown in Fig. 16 for different levels of pretensioning forces (bpl).

It is important to note that the beam with $\rho/\rho_b > 1.0$ failed due to crushing of concrete while those with $\rho/\rho_b < 1.0$

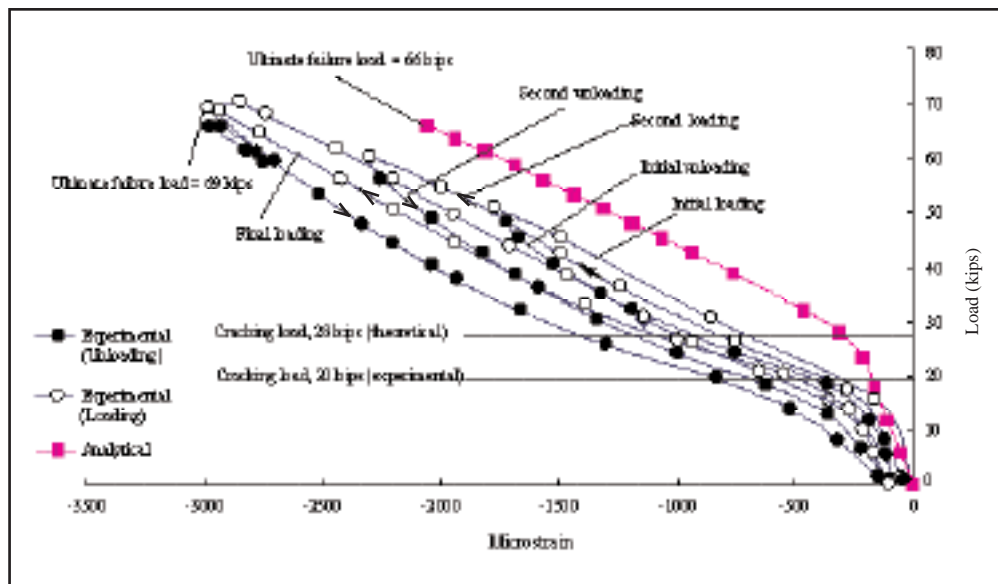


Fig. 15. Load versus strain in top flange at midspan of Box Beam DN2.

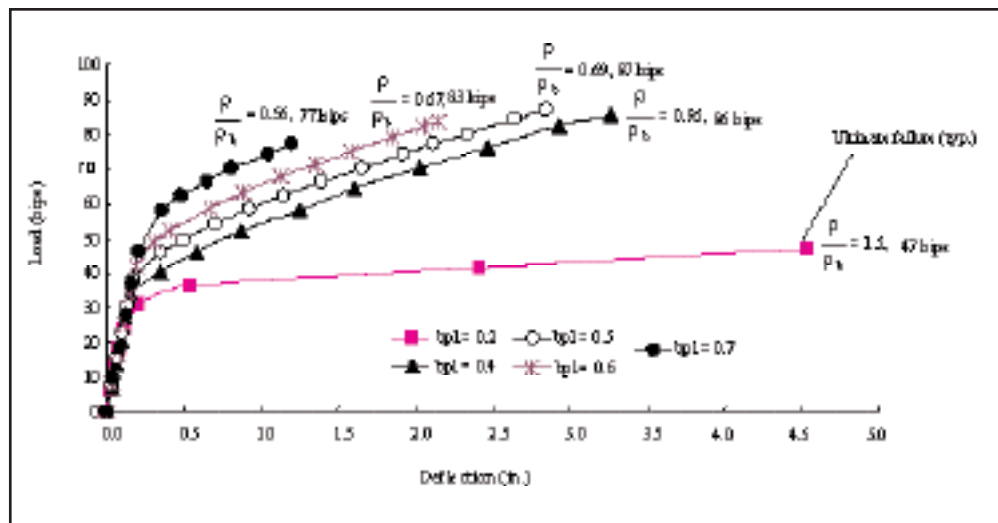


Fig. 16. Effect of level of pretensioning forces (bpl) on the load-versus-deflection response of box beam at $upl = 0.7$.

failed due to rupture of pretensioning tendons. A pretensioning force level $bpl = 0.4$ resulted in the ultimate load of 86 kips (383 kN) of box beam identical to that for $bpl = 0.5$. However, this level of pretensioning force ($bpl = 0.4$) resulted in a higher deflection corresponding to the ultimate failure load in comparison to that for the pretensioning force level, $bpl = 0.5$.

The difference in the ultimate load responses for $bpl = 0.4$ and 0.5 is attributed to the almost balanced-section behavior of box beam for $bpl = 0.4$ and under-reinforced box beam behavior for $bpl = 0.5$. The increase in the $bpl > 0.5$ reduces the load-carrying capacity of the beam. The lowest load-carrying capacity was observed for $bpl = 0.7$ due to significantly under-reinforced box beam behavior at this level of pretensioning forces.

For a particular load, reinforcement ratio ($\rho = 0.0034$), and for a constant level of pretensioning force ($bpl = 0.5$),

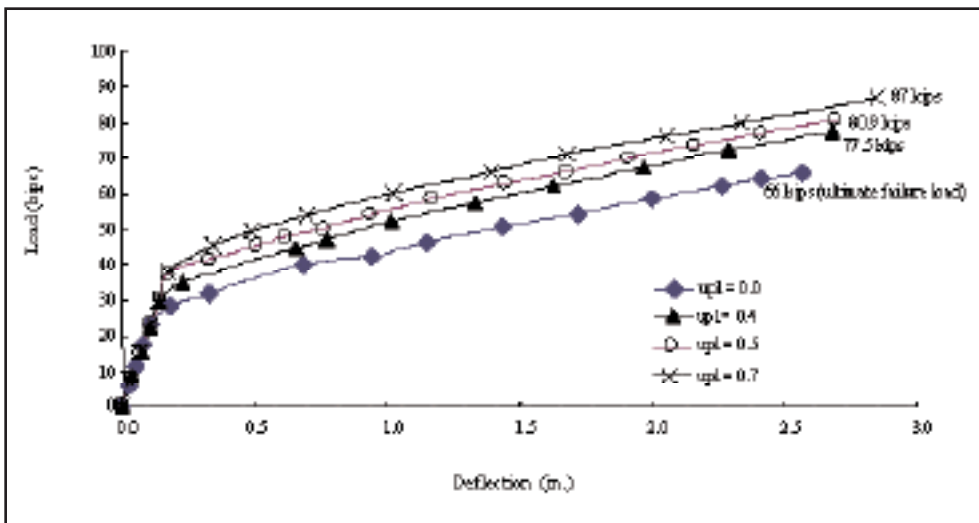


Fig. 17. Effect of level of unbonded post-tensioning forces (upl) on the load-deflection response of box beams at $bpl = 0.5$.

deflection is higher for the lower unbonded post-tensioning prestress level than that for the higher level of post-tensioning forces (see Fig. 17). The higher level of unbonded post-tensioning also results in higher load-carrying capacity, provided that the unbonded tendons remain intact at the ultimate failure of the box beam. The load value shown in Fig. 17 corresponding to each response curve represents the ultimate failure load of the beam for the corresponding unbonded post-tensioning force level (upl).

CONCLUSIONS

Based on the experimental and analytical evaluations of the box beams reinforced and prestressed using bonded and unbonded CFRP tendons, the following conclusions are drawn:

1. The measured decompression loads for Beams DP1, DN2, and LP3 are 31.5, 18.8, and 32.0 kips (140, 83.6, and 142 kN), respectively. The corresponding losses in pretensioning forces in tendons of Beams DP1, DN2, and LP3 are 13.6, 8.3, and 10.2 percent, respectively.

2. The combination of bonded and unbonded prestressing increased the ultimate load of the box beam by about 26 percent in comparison to the beam with non-prestressed unbonded post-tensioning tendons. The beam with non-prestressed unbonded post-tensioning tendons, however, resulted in 36 percent higher energy ratio in comparison to the corresponding beam prestressed using both the pretensioning and unbonded post-tensioning tendons.

3. Comparison of the analytical and experimental results validated the accuracy of the developed computer program for CFRP prestressed concrete box beams. Minor differences in the analytical and experimental results were primarily due to loading and unloading cycles applied to the box beam and due to the assumptions made in the equations.

4. For a given level of unbonded post-tensioning forces, the level of pretensioning forces in the bonded tendons affects the flexural load-versus-deflection response, ultimate load, and failure modes of the box beams.

5. The effective pretensioning force level (bpl) of 0.4 in conjunction with post-tensioning force level (upl) of 0.7 resulted in a maximum ultimate load-carrying capacity, with crushing of concrete prior to rupture of bonded pretensioning tendons. The pretensioning levels (bpl) greater than 0.4 resulted in rupture of bonded pretensioning tendons before crushing of concrete.

6. For a fixed value of pretensioning force level and reinforcement ratio, the higher level of unbonded post-tensioning forces results in the higher load-carrying capacity of the box beam provided the unbonded tendons remain intact until ultimate failure of the box beam.

RECOMMENDATIONS

The prestressing of box beams using internal bonded pretensioning tendons in conjunction with internal unbonded post-tensioning tendons is recommended to maximize the load-carrying capacity of the beam. The effective pretensioning force level (bpl) should be between 0.3 and 0.4, while the corresponding level of forces in unbonded post-tensioning tendons should be about 0.7 if crushing of the concrete is the desired mode of failure. These levels of forces in bonded pretensioning and unbonded post-tensioning tendons could significantly increase the load-carrying capacity of box beams and preclude the early failure of box beams caused by rupture of bonded pretensioning tendons prior to crushing of the concrete.

ACKNOWLEDGMENTS

This research was funded by the Ohio Department of Transportation (ODOT), the Federal Highway Administration (FHWA) under Contract No. 14718, and the National Science Foundation under Grant No. CCMS 9900809. The authors would like to thank the following ODOT personnel for their help and suggestions: Monique R. Evans, Brad Fagrel, Tim Keller, Vikram Dalal, Valerie Frank, and Karen Panell of the Office of Research and Development and the Office of Structural Engineering. The support of Dr. P. N. Balaguru of the National Science Foundation is greatly appreciated. The authors are also grateful for the support of Tokyo Rope Mfg. Co. Ltd. (Mr. T. Enomoto) and Mitsubishi Chemical Functional Products, Inc. (Mr. K. Yagi).

Finally, the authors extend their thanks to the PCI JOURNAL reviewers for their constructive comments.

The views and conclusions presented in this paper represent those of the authors and not necessarily those of ODOT, FHWA, and NSF.

REFERENCES

1. ACI Subcommittee 440I, "Guidelines for Prestressing Concrete Structures with FRP Tendons," Draft, American Concrete Institute, Farmington Hills, MI.
2. Naaman, A. E., Tan, K. H., Jeong, S. M., and Alkhairi, F. M., "Partially Prestressed Beams with Carbon Fiber Composite Cable Strands: Preliminary Tests on Strands," *Fiber-Reinforced-Plastic Reinforcement for Concrete Structures*, SP-138, American Concrete Institute, Farmington Hills, MI, 1993, pp. 441-464.
3. Yonekura, A., Tazawa, E., and Nakayama, H., "Flexural and Shear Behavior of Prestressed Concrete Beams Using FRP Rods as Prestressing Tendons," *Fiber-Reinforced-Plastic Reinforcement for Concrete Structures*, SP-138, American Concrete Institute, Farmington Hills, MI, 1993, pp. 525-548.
4. Abdelrahman, A., Rizkalla, S. H., and Tadros, G. B., "Deformability of Flexural Concrete Members Prestressed with FRP Tendons," *Proceedings of the Third International Symposium on Non-Metallic (FRP) Reinforcement for Concrete Structures*, V. 2, Sapporo, Japan, October 1997, pp. 767-774.
5. Zou, X. W., Gowripalan, N., and Gilbert, R. I., "Short-Term Behavior of Concrete Beams Prestressed with CFRP Tendons," *Proceedings of the Third International Symposium on Non-Metallic (FRP) Reinforcement for Concrete Structures*, V. 2, Sapporo, Japan, October 1997, pp. 743-750.
6. Kato, T., and Hayashida, N., "Flexural Characteristics of Prestressed Concrete Beams with CFRP Tendons," *Fiber-Reinforced-Plastic Reinforcement for Concrete Structures*, SP-138, American Concrete Institute, Farmington Hills, MI, 1993, pp. 419-440.
7. Maissen, A., and de Semet, C. A. M., "Comparison of Concrete Beams Prestressed with Carbon Fiber-Reinforced Plastic and Steel Strands," *Non-Metallic (FRP) Reinforcement for Concrete Structures: Proceedings of the Second International Conference on Advanced Composite Materials for Bridges and Structures*, ACMBS-II, Montreal, Quebec, Canada, 1995, pp. 227-234.
8. Naaman, A. E., and Jeong, S. M., "Structural Ductility of Concrete Beams Prestressed with FRP Tendons," *Non-Metallic (FRP) Reinforcement for Concrete Structures: Proceedings of the Second International RILEM Symposium (FRPRCS-2)*, Ghent, Belgium, August 23-25, 1995, pp. 379-386.
9. Grace, N. F., Enomoto, T., and Yagi, K., "Behavior of CFCC and CFRP Leadline Prestressing Systems in Bridge Construction," *PCI JOURNAL*, V. 47, No. 3, May-June 2002, pp. 90-103.
10. Grace, N. F., "Response of Continuous CFRP Prestressed Concrete Bridges Under Static and Repeated Loadings," *PCI JOURNAL*, V. 45, No. 6, November-December 2000, pp. 84-102.
11. Grace, N. F., and Singh, S. B., "Design Approach for CFRP Prestressed Concrete Bridge Beams," *ACI Structural Journal*, V. 100, No. 3, May-June 2003, pp. 365-376.
12. Grace, N. F., and Singh, S. B., "Unified Analysis and Design Approach for CFRP Prestressed Concrete Bridge Girders," *Proceedings of the 10th U.S.-Japan Conference on Composite Materials*, Stanford, CA, September 16-18, 2002, pp. 328-335.
13. Grace, N. F., Enomoto, T., Abdel-Sayed, G., Yagi, K., and Collavino, L., "Experimental Study and Analysis of a Full-Scale CFRP/CFCC Double-Tee Bridge Beam," *PCI JOURNAL*, V. 48, No. 4, July-August 2003, pp. 120-139.
14. Grace, N. F., Navarre, F., Nacey, R. B., Bonus, W., and Collavino, L., "Design-Construction of Bridge Street Bridge — First CFRP Bridge in the United States," *PCI JOURNAL*, V. 47, No. 5, September-October 2002, pp. 20-35.
15. Diversified Composites Inc. (DCI), "Product Manual of Diversified Composites, Inc.," Erlanger, KY, 2002.
16. Mitsubishi Chemical Corporation (MCC), "Leadline™ Carbon Fiber Tendons/Bars," Product Manual, Tokyo, Japan, 1994.
17. Tokyo Rope Mfg. Co. Ltd., "Carbon Fiber Composite Cables (CFCC)," Product Manual, Tokyo, Japan, 1993.

APPENDIX — NOTATION

| | |
|--|--|
| <p>A_{fi} = cross-sectional area of reinforcement of a particular material (positive for tensile reinforcement and negative for compression reinforcement)</p> <p>A_{fu} = total cross-sectional area of post-tensioning tendons</p> <p>A_{pb} = total cross-sectional area of pretensioning bonded tendons</p> <p>A_{pn} = total cross-sectional area of non-prestressing rods provided in tension zone</p> <p>A_{pnf} = total cross-sectional area of non-prestressing rods provided in compression zone</p> <p>b = flange width of beam</p> <p>C = resultant compression force in concrete of compression zone</p> <p>C_R = sum of resultant compression force in concrete and force in compression non-prestressing rods</p> <p>d = distance from extreme compression fiber to centroid of tension reinforcement</p> <p>\bar{d} = distance of center of gravity of resultant compression force from extreme compression fiber</p> <p>d_m = distance of centroid of bottom prestressing tendons from extreme compression fiber</p> <p>f_{bi} = total stress in an equivalent tendon of a specific material at balanced condition</p> <p>f_{fu} = specified tensile strength of bonded pretensioning tendons</p> <p>f_{pbb} = flexural stress in equivalent bonded pretensioning tendons at balanced condition</p> <p>f_{pbm} = total stress in pretensioning tendon of bottom row</p> <p>f_{pnb} = total stress in a non-prestressing rod of bottom row</p> <p>f_{pnbb} = flexural stress in equivalent non-prestressing rods provided in tension zone at balanced condition</p> <p>f_{pnfb} = flexural stress in equivalent non-prestressing rods provided in compression zone at balanced condition</p> <p>f_{pnt} = total stress in non-prestressing rod located in top flange of box beam</p> <p>f_{pu} = total stress in unbonded tendon</p> <p>f_{pub} = flexural stress in equivalent unbonded tendons at</p> | <p>balanced condition</p> <p>F_{pbm} = resultant force in pretensioning tendons</p> <p>F_{pi} = resultant initial effective pretensioning force</p> <p>F_{pnb} = resultant force in non-prestressing rods of tension zone</p> <p>F_{pnt} = resultant force in non-prestressing rod of compression zone</p> <p>F_{pui} = resultant initial effective post-tensioning force</p> <p>F_{pu} = total force in unbonded post-tensioning tendons</p> <p>F_R = resultant of tensile forces in bonded and unbonded tendons</p> <p>m = total number of layers of bonded pretensioning tendons</p> <p>n = depth to neutral axis from extreme compression fiber</p> <p>p = total number of reinforcing materials</p> <p>α_i = ratio of total stress in equivalent tendon of particular material at balanced condition to specified strength of pretensioning tendon</p> <p>β_1 = factor defined as ratio of depth of equivalent rectangular stress block to distance from extreme compression fiber to neutral axis</p> <p>f'_c = specified compressive strength of concrete</p> <p>f_{fu} = specified tensile strength of bonded prestressing tendons</p> <p>ϵ_{cu} = ultimate compressive strain in concrete (0.003)</p> <p>ϵ_{fu} = specified ultimate strain of pretensioning tendons</p> <p>ϵ_{pbm} = total strain in pretensioning tendon of bottom row</p> <p>ϵ_{pbmi} = initial prestressing strain in bonded prestressing tendons of mth row ($m = 1$)</p> <p>ϵ_{pnb} = total strain in non-prestressing tendon of bottom flange</p> <p>ϵ_{pnt} = total strain in non-prestressing tendon of top flange</p> <p>ϵ_{pui} = initial strain in unbonded post-tensioning tendons</p> <p>$\Delta\epsilon_{pu}$ = flexural strain in unbonded post-tensioning tendons</p> <p>ϵ_{fbm} = flexural strain in pretensioning tendons</p> <p>ρ = reinforcement ratio</p> <p>ρ_b = balanced ratio</p> |
|--|--|